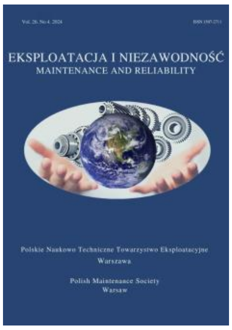

Eksploatacja i Niezawodnosc – Maintenance and Reliability

Volume 26 (2024), Issue 4

journal homepage: http://www.ein.org.pl

Article citation info:
Ge H, Wang C, Guo A, Zhang C, Zhao Z, Yang M, Wear state identification of ball screw meta action unit based on parameter optimization VMD and improved Bilstm, Eksploatacja i Niezawodnosc – Maintenance and Reliability 2024: 26(4) http://doi.org/10.17531/ein/191461

Wear state identification of ball screw meta action unit based on parameter optimization VMD and improved Bilstm

Indexed by: Web of Science Group

Hongyu Ge[a], Cangfu Wang[a,*], Anxiang Guo[a], Chuanwei Zhang[a], Zhan Zhao[a], Manzhi Yang[a]

[a] School of Mechanical Engineering, Xi'an University of Science and Technology, China

Highlights

- Tent chaotic map and adaptive cosine algorithm are used to improve the Northern Goshawk optimization algorithm.
- The parameters of VMD are optimized by using the improved Northern Goshawk optimization algorithm.
- A wear state recognition model based on Bayesian optimization Bilstm hyperparameters was constructed.

Abstract

Aiming at the problem that the wear feature information of the ball screw meta-action unit is easily disturbed by noise and the wear state recognition accuracy is not high, a wear state recognition method based on parameter optimization VMD and improved Bilstm was proposed.Firstly, Tent chaotic mapping and adaptive positive cosine algorithm are used to improve Northern Goshawk Optimisation Algorithm (INGO); Secondly, the INGO-VMD was used to decompose the collected vibration signals. The power spectrum entropy, alignment entropy and fuzzy entropy of the IMF components with large correlation after decomposition are calculated to construct the feature information matrix. Finally, the described feature information matrix with labels was input into the Bayesian Optimization Bilstm network model for training, and the Softmax classifier was used to classify the wear state categories. In order to verify the superiority of the proposed method, it is compared with VMD-Lstm, VMD-Bilstm and VMD-Bo-Bilstm models, and the results show that the designed method has higher recognition accuracy.

Keywords

ball screw, VMD parameter optimization, Bilstm model improvement, wear condition recognition

1. Introduction

Ball screw meta-action unit is the core functional unit in CNC machine tools and other high-end mechanical equipment[1, 2], when it is in a long period of time, high-intensity machining conditions, the internal movement of the vice (gears, nut vice, etc.) inevitably wear[3], until different degrees of failure. In turn, the machining accuracy of the machine tool is adversely affected, which ultimately leads to the poor quality of the processed products, causing serious economic losses to the enterprise[4, 5]. Therefore, it is of practical significance to carry out the research on the identification of the wear state of the ball screw meta-action unit to avoid the occurrence of safety accidents.

Existing research on ball screw wear state identification is usually divided into physical model-based approaches and data-driven approaches. The former needs to understand the physical mechanism of the device under test, analyse the mechanism of wear occurrence and find out the intrinsic law of degradation of its operating state, but it is difficult to establish a more accurate mathematical model[6, 7]. The latter is mainly through the use of sensing technology to obtain the historical response data of its operating state, mine the characteristic information of wear in the response data, and then achieve the pattern matching

(*) Corresponding author.
E-mail addresses: H. Ge, ghy-xkd@xust.edu.cn, C. Wang (ORCID: 0009-0003-8416-7114) 2060638837@qq.com, A. Guo, 1694948586@qq.com, C. Zhang. zhangcw@xust.edu.cn, Z. Zhao, 5649358372@qq.com, M. Yang, xkdymz@xust.edu.cn,

between the characteristic information and the wear state with the help of machine learning and other means, so as to classify and identify the current wear state of the screw [8, 9]. It can be roughly divided into data acquisition, wear feature extraction and wear state recognition[10], among which, wear feature extraction and wear state recognition are the core of the problem. Especially when the wear degree changes weakly and is subject to external interference, the work of wear feature information extraction and wear state recognition is difficult to be carried out smoothly. Therefore, how to choose the appropriate wear feature extraction method and wear state recognition method is particularly important.

At present, a lot of research has been done at home and abroad on the wear feature extraction techniques for mechanical equipment, and most of them take the form of signal processing and feature quantisation for the extraction of wear features, and typical methods include Short Time Fourier Transform (STFT) [11, 12], Wavelet Transform (WT) [13, 14], Empirical mode decomposition (EMD)[15, 16], and Variable Mode Decomposition (VMD)[17, 18], etc. Although these methods are widely used, they still have certain shortcomings. Among them, the time-frequency domain resolution of STFT cannot be dynamically adjusted with the frequency level, WT needs to pre-select the basis function and has a high dependence on it, and EMD has the problem of end effect and mode aliasing, which also affects the accuracy of wear state recognition. In view of the existing problems of EMD, Dragomiretskiy K et al.[19] proposed the VMD method, which not only eliminates the mode aliasing problem of EMD, but also can obtain the IMF component with higher signal-to-noise ratio, and the final extracted features are more obvious. However, the effect of VMD decomposition is affected by the number of modes and penalty factor in the algorithm, and it is generally difficult to select the optimal combination of the number of modes and penalty factor based on experience[20]. In order to optimize the two built-in parameters of VMD, Zhou et al.[21]used the method based on peak spectrum clustering and center frequency to determine the optimal range of the number of VMD modes and the penalty factor. Li et al.[22] used Northern goshawk optimization (NGO) algorithm to optimize the number of modes and penalty factor of VMD, Xu et al.[23] used NGO to optimize the number of modes of VMD. The optimal parameter combination shows a good VMD decomposition effect, but the NGO algorithm is easily affected by the uneven distribution of the initial population in the process of optimization, resulting in a local optimum problem, which will have a negative impact on the optimization effect of the algorithm[24].

On the other hand, in recent years, a series of achievements have been made in the research of mechanical equipment wear state recognition methods. S. Laddada et al.[25] proposed a compound method combining complex continuous wavelet transform and improved extreme learning machine to identify the wear state of CNC machine tools. By generating a performance degradation model, the health index was obtained, and then the wear state was identified. Ou et al.[26] proposed a method for intelligent recognition of tool wear state by stack denoising autoencoder (SDAE) based on online sequential Extreme Learning Machine (OS-ELM). Zhang et al.[27] According to the advantages of Long short-term memory (LSTM), which can effectively extract the sensitive features of time series data, the fault diagnosis of gear box is realized. However, the LSTM model can only process the data one-way. It is not possible to fully extract the internal connection of data information in time series[28]. Therefore, bidirectional long short-term memory (Bilstm) is improved on the basis of LSTM[29]. The Bilstm network model enables the network to process data bidirectionally. Thus, the correlation between historical information and current data information and the ability of state recognition can be improved[30, 31]. However, it is difficult to select the value of hyperparameter in Bilstm model[32].

Based on the above analysis, this paper takes the ball screw meta-action unit which is common in CNC machine tools as the main research object, takes the vibration response signal of the screw wear state as the data basis, and uses the decomposition method of improved NGO to optimize VMD parameters to decompose the vibration signal of the screw, so as to obtain a good decomposition effect. Then, on the basis of signal decomposition, the relevant IMF components are screened and the corresponding wear features are extracted to characterize the change of the wear state of the lead screw. The extracted wear features are used to construct the feature information matrix, which is used as the input of the improved Bilstm model to realize the wear state recognition of the lead screw in the ball screw meta-action unit.

2. Construction of experimental platform and information collection

2.1. Experimental platform construction

Ball screw meta action unit is a CNC machine tool and other high-end manufacturing equipment in the key transmission unit, the form of movement is mainly through the screw, nut and nut raceway between the rolling body back and forth circular spiral movement, so that the rotary motion of the screw into the linear motion of the table, with high transmission efficiency, good reliability, positioning accuracy and other characteristics. Its structural composition includes five parts: input parts, execution parts, intermediate parts, support parts and fasteners[33]. Taking the wear state recognition of middleware ball screw as an example, this paper establishes an experimental platform for collecting vibration response signals under different wear states to provide data support for subsequent wear feature extraction. The composition of its experimental equipment is shown in Fig. 1.

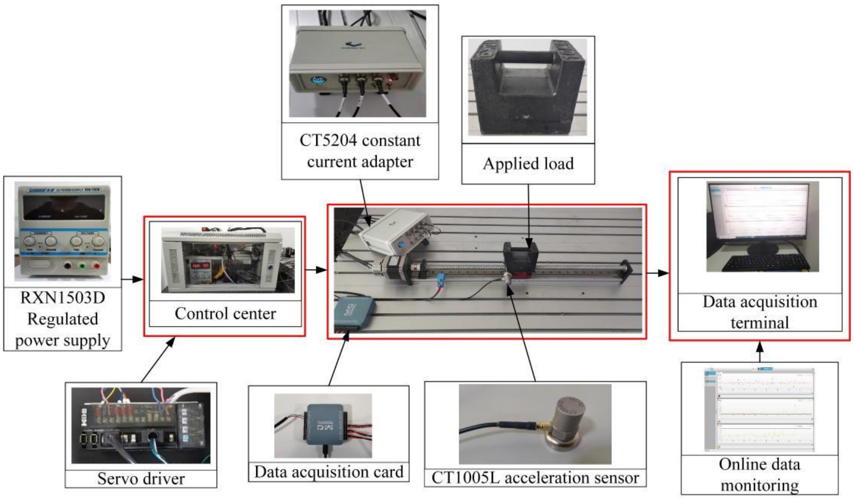

Fig. 1. Lead screw wear test equipment composition diagram.

2.2. Vibration information Collection

In general, the more serious the degree of wear of the screw, the more intense the vibration, and the vibration frequency will also change with the intensification of wear. Based on this, this paper collects the vibration data of screw wear under continuous operation by installing vibration sensors on the nut pair of the output member of the meta-action unit, and then mines the characteristic information related to the change of screw wear state, establishes the mapping relationship between the vibration data and the wear state, and ultimately realises the recognition of the wear state of the screw of the output member of the ball screw meta-action unit. The specific steps of vibration data acquisition are as follows:

(1) Screw selection and parameter setting. In the experimental process of information acquisition, the motor speed is set to 100r/min and the room temperature is about 20℃. The diameter of the selected ball screw is 16mm, the lead is 10mm, the ball diameter is 6.35mm, and the maximum horizontal load is 22kg and vertical load is 20kg.

(2) Design of test scheme. Based on the influence of wear time and lubrication conditions on the wear degree of the ball screw, an experimental scheme for ball screw operation under different wear time and lubrication conditions was established, as shown in Table 1. Among them, in the phase of non-lubrication accelerated wear of the ball screw, based on the maximum vertical load of the ball screw pair used in this experiment is 20kg, therefore, a weight of 10kg is fixed on the ball screw nut pair, that is, a load of 100N is applied to accelerate the performance degradation process of the ball screw (g=10N/kg in this paper). Thus, the data characteristics under different wear durations can be better distinguished.

(3) Establishment of acquisition system. Paste the sensor in the upper position of the output piece to complete the connection between the sensor, data acquisition card, signal acquisition software and computer.

(4) Acquisition of vibration information under lubrication conditions. During the experiment, the sampling frequency was set to 5000Hz, and one set of data was collected every five strokes of the screw. At the beginning of the operation of the

screw, the screw is fully lubricated every 5 minutes, and the possibility of failure of the screw during this movement is low, so 40 sets of data are collected as samples in the good health condition interval.

(5) Due to the long life of the ball screw, it is difficult to obtain the life cycle data of the ball screw running to failure under normal operating conditions. Therefore, in this paper, the wear process of the ball screw is first accelerated by increasing the load to make the ball screw in a non-lubricated state. Secondly, on the basis of adding load and no lubrication, different wear states were defined according to the wear time of the ball screw, that is, different wear states of the ball screw were simulated by changing the wear time, so the data acquisition method of interval sampling was selected in the experiment. That is, the vibration data corresponding to the wear time of 50min, 120min, 180min and 400min were collected respectively, and the data were collected every 5 strokes. Finally, 140 sets of data were collected as sample data for each of the four wear states.

Table 1. Experimental programme for ball screw operation.

Label	Type of screw	Wear hours	Operating conditions	Performance status
1	Brand new	0min	Lubricated every 5 minutes	Good health
2	Non-new	50min	No lubrication	50min poor lubrication
3	Non-new	120min	No lubrication	120min poor lubrication
4	Non-new	180min	No lubrication	180min poor lubrication
5	Non-new	400min	No lubrication	400min poor lubrication

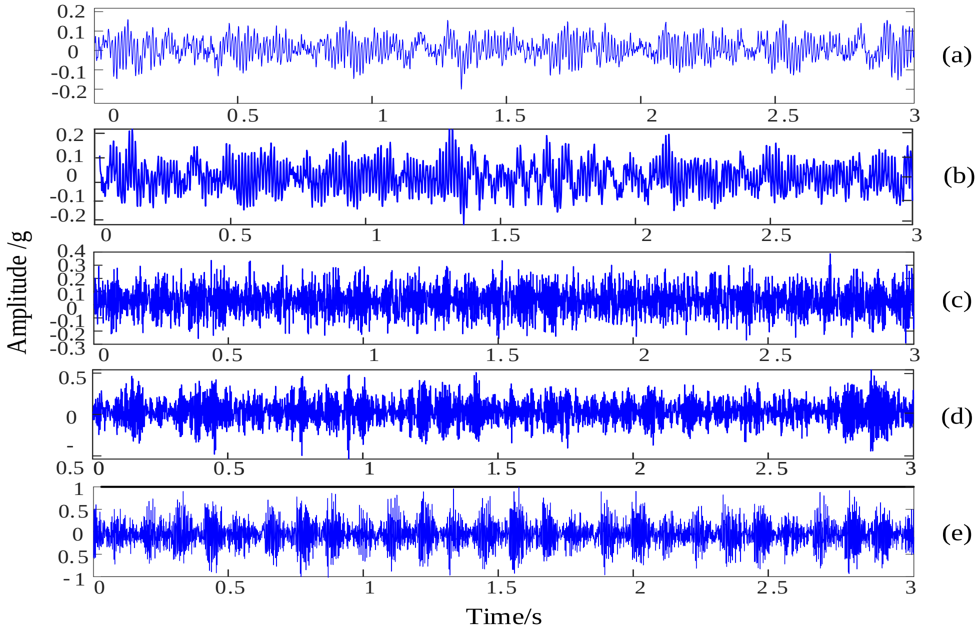

(a) Good health; (b) 50min poor lubrication; (c) 120min poor lubrication; (d) 180min poor lubrication; (e) 400min poor lubrication

Fig. 2. Time-domain waveform of vibration signal for ball screw wear.

Figure 2 shows the vibration signals collected by the acceleration sensor under the five performance states of the ball screw. Comparing the vibration signals under each state, it can be seen that the amplitude of the vibration signal changes as the ball screw continues to wear under the condition of no lubrication, so the vibration signal of the ball screw can be used to monitor its wear state.

3. Wear feature extraction

Although there are differences in the frequencies of the vibration signals under different wear durations and lubrication conditions, it is not possible to distinguish the corresponding wear types from the specific vibration signals. Therefore, further analyses of the acquired vibration signals are required to extract different wear feature information and thus accurately identify the corresponding wear condition categories.

3.1. VMD parameter optimization based on improved NGO

3.1.1. Improvement of NGO algorithm

The vibration signal of the ball screw meta-action unit has the characteristics of non-smoothness, non-linearity and weak change of wear feature information, and it is difficult for conventional signal processing methods to meet the accurate extraction of wear feature information.VMD can not only realise the adaptive decomposition of non-smooth signals, but also effectively inhibit the occurrence of the modal overlapping of the traditional methods, and has good robustness. Therefore, in this paper, VMD is used to decompose the vibration signal of the ball screw meta-action unit to achieve the accurate extraction of wear feature information. However, VMD needs to set the number of modes k and the penalty factor α when decomposing the signals, which may lead to over-decomposition or under-decomposition of the modes if they are not set properly. Based on this, considering the mutual influence between parameters k and α, this paper uses the improved NGO to optimise the VMD to select the optimal combination of parameters k and α. The VMD can be used for the decomposition of vibration signals.

NGO is an intelligent optimization algorithm proposed by Mohammad Dehghani et al.[34] researchers in 2021. The algorithm simulates the behavior of northern goshowl to hunt prey. Its hunting behavior can be divided into prey recognition stage and pursuit and escape stage.

(1) Prey identification phase

In this phase the northern goshawk selects a prey at random and pursues it rapidly, this phase is a global search aimed at identifying the best area with the mathematical expression:

$$P_i = X_k, i = 1,2,\dots,N, k = 1,2,\dots,i-1,i+1,N \tag{1}$$

$$X_i = \begin{cases} x_i^{new,P_1}, & F_i^{new,P_1} < F_i \\ X_i, & F_i^{new,P_1} \geq F_i \end{cases} \quad x_{i,j}^{new,p_1} = \begin{cases} x_{i,j} + q(p_{i,j} - Ex_{i,j}), F_{P_i} < F_i \\ x_{i,j} + q(x_{i,j} - p_{i,j}), F_{P_i} \geq F_i \end{cases} \tag{2}$$

Where P_i is the position of the prey of the i th northern goshawk, F_{P_i} is the value of the objective function, k is a random integer between $[1,N]$, x_i^{new,P_1} denotes the new state of the i th northern goshawk, $x_{i,j}^{new,p_1}$ denotes the new state of the i th northern goshawk in the j th dimension, F_i^{new,P_1} is the value of the objective function in the new state of the i th northern goshawk, q is a random number that belongs to $[0,1]$, E is 1 or 2, and q and E are random numbers used for the generation of the NGOs in the search and iterative updating. random numbers in the update.

(2) Pursuit and escape phase

When the prey is pursued by the northern goshawk, the prey instinctively tries to escape, and the northern goshawk needs to pursue the prey further. Assuming that the hunting is within a radius of R, the mathematical expression of this stage is as follows:

$$x_{i,j}^{new,p_2} = x_{i,j} + R(2r-1)x_{i,j} \tag{3}$$

$$R = 0.02\left(1 - \frac{t}{t_{max}}()\right) \tag{4}$$

$$X_i = \begin{cases} x_i^{new,P_2}, & F_i^{new,P_2} < F_i \\ X_i, & F_i^{new,P_2} \geq F_i \end{cases} \tag{5}$$

Where, t is the current iteration number, t_{max} is the maximum iteration number, x_i^{new,P_2} represents the new state of the i th northern goshawk updated in the second stage, c represents the new state of the i th northern Goshawk in the second stage in the j th dimension, and F_i^{new,P_2} is the objective function value in the second stage.

The aforementioned NGO algorithm can be utilized to optimize the parameters of VMD in order to achieve a superior decomposition effect for extracting the wear characteristics of the lead screw. Nevertheless, the NGO algorithm does have certain limitations during the optimization process. Therefore, this paper proposes an enhancement to the traditional NGO algorithm by incorporating Tent chaotic mapping and sine-cosine algorithm with adaptive weights, resulting in the improved INGO algorithm. The specific steps for improvement are as follows:

(1) In order to address the issue of random distribution of the initial solution in the population initialization process of the NGO algorithm, this paper leverages the benefits of randomness, ergodicity, and regularity offered by chaotic sequences to generate individual solution sequences at the initial stage of the NGO algorithm. This approach aims to achieve a more even distribution of individuals within the population. The population representation for the NGO initialized with chaotic sequence based on Tent is as follows:

$$z_{j+1}^{i}=\begin{cases}2z_j^i, & 0\le z_j^i\le \frac{1}{2}\\ 2(1-z_j^i), & \frac{1}{2}<z_j^i\le 1\end{cases} \tag{6}$$

Where, z_j^i is the chaotic sequence, $i=1,2\cdots,N$ is the population size number of the northern goshawk, $j=1,2,\cdots,d$ is the dimension of the solution.

However, Tent chaotic sequence has unstable periodic points in the process of iteration. In order to avoid falling into unstable periodic points, a random number $rand(0,1)\cdot\frac{1}{N_r}$ is introduced to perturb the sequence based on the original expression, and the improved expression of Tent chaotic sequence is as follows:

$$z_{j+1}^{i}=\begin{cases}2z_j^i+rand(0,1)\cdot\frac{1}{N_r}, & 0\le z_j^i\le \frac{1}{2}\\ 2(1-z_j^i)+rand(0,1)\cdot\frac{1}{N_r}, & \frac{1}{2}<z_j^i\le 1\end{cases} \tag{7}$$

Select d initial individuals and substitute them into Equation (7) to generate a chaotic sequence, and then reverse map them to the solution space to obtain the chaotic initial solution of NGO:

$$x'_{ij}=lb_{ij}+(ub_{ij}-lb_{ij})x_{ij} \tag{8}$$

Where, ub_{ij} and lb_{ij} are the upper and lower bounds of feasible solutions, respectively.

(2) In view of the situation that the NGO algorithm is trapped in a local optimum, the sine cosine algorithm is introduced to improve the prey identification stage of NGO, so as to improve the global search ability of NGO, and finally obtain the overall optimal solution. The individual position update formula in the optimization process is as follows:

$$x_{i,j}^{new,p_1}=\begin{cases}x_{i,j}+r_1\sin r_2\left|r_3x_{best}-x_{i,j}\right|, r_4<0.5\\ x_{i,j}+r_1\cos r_2\left|r_3x_{best}-x_{i,j}\right|, r_4\ge 0.5\end{cases} \tag{9}$$

Where, r_1 is the adjustment parameter of sine and cosine algorithm, r_2 is the random number between $[0,2\pi]$, determines the moving direction and distance of the updated solution, r_3 is the random number between $[0,2]$, which is mainly used to control the influence degree of the current solution on the update of the next solution, r_4 is the random number between $[0,1]$, which determines the iterative update of the sine and cosine function part in Equation (9).

In the above individual position update iteration process, the parameter r_1 plays a major role, and its expression formula is as follows:

$$r_1=a\left(1-\frac{t}{t_{max}}()\right) \tag{10}$$

Where, a is usually a constant; in this paper, $a=1$, t is the current iteration number, and t_{max} is the maximum iteration number.

It can be seen from Equation (10) that r_1 is a linearly decreasing function, and its value decreases with the increase of the number of iterations, which is not conducive to balancing the ability of global search or local optimization of NGO algorithm. To this end, this paper improves r_1, and the change curve of r_1 after improvement is shown in Figure 3. It can be seen that the decreasing speed is slow in the early stage, which is conducive to the global search of the algorithm, and the decreasing speed is fast in the later iteration, which enhances the local optimization ability of the algorithm. The improvement formula is:

$$r'_1=a\left(1-\left(\frac{t}{t_{max}}()^{\cos(\frac{t}{10t_{max}})}\right)\right) \tag{11}$$

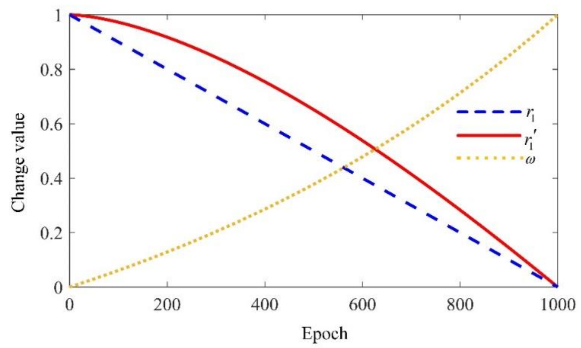

Fig. 3. Parameter variation curve of sine cosine algorithm.

Considering that the individual position of the current solution depends heavily on the individual position of the previous iteration solution in the whole search process of the sine cosine algorithm, this paper introduces an adaptive weight to replace the constant inertia weight of the current solution. The new adaptive weight formula is as follows:

$$\omega=\frac{e^{\frac{t}{t_{max}}}}{e-1} \tag{12}$$

The change of weight curve is shown in Fig. 3. In the early stage of optimization, a small weight reduces the influence of the current solution on the optimization iterative update solution, thereby improving the development ability of the algorithm. Finally, the new individual position update formula is obtained as follows:

$$x_{i,j}^{new,p_1}=\begin{cases}\omega x_{i,j}+r_1'\sin r_2\left|r_3x_{best}-x_{i,j}\right|, r_4<0.5\\ \omega x_{i,j}+r_1'\cos r_2\left|r_3x_{best}-x_{i,j}\right|, r_4\ge 0.5\end{cases} \tag{13}$$

3.1.2. Performance test of INGO algorithm

To evaluate the feasibility and performance of the improved NGO algorithm in this paper, Dung Beetle Optimization (DBO), Golden Eagle Optimizer (GEO), Beluga Whale Optimization (BWO) algorithm and the standard NGO algorithm are compared in terms of comprehensive performance on four more common test functions shown in Table 2, where $f_1(x)$ and $f_2(x)$ are unimodal functions, $f_3(x)$ and $f_4(x)$ are multimodal functions. In order to ensure fairness among the five algorithms, the maximum number of iterations, population number and dimension of each algorithm are set the same. The specific parameters are as follows: the maximum number of iterations is 1000, the population number is 100, and the dimension is 30.

Table 2. Four more common test functions.

Benchmark functions	Range of search	Theoretical value
$f_1(x) = \sum_{i=1}^{n} {x_i}^2$	[-100,100]	0
$f_2(x) = \sum_{i=1}^{n} \lvert x_i \rvert + \prod_{i=1}^{n} \lvert x_i \rvert$	[-10,10]	0
$f_3(x) = \sum_{i=1}^{n} -x_i \, sin\left(\sqrt{\lvert x_i \rvert}\right)$	[-500,500]	12569.5
$f_4(x) = -20\, exp(-0.2\sqrt{\frac{1}{n}\sum_{i=1}^{n} {x_i}^2}) - exp(\frac{1}{n}\sum_{i=1}^{n} cos(2\pi x_i)) + 20 + e$	[-32,32]	0

The optimization results of the five algorithms on the four test functions are shown in Fig 4. From the test results in Fig 4, it can be seen that INGO algorithm has higher accuracy and faster convergence than the other four algorithms, which is due to the introduction of Tent chaotic map and improved sine cosine algorithm. Thus, the feasibility and superiority of the INGO algorithm designed in this paper are verified.

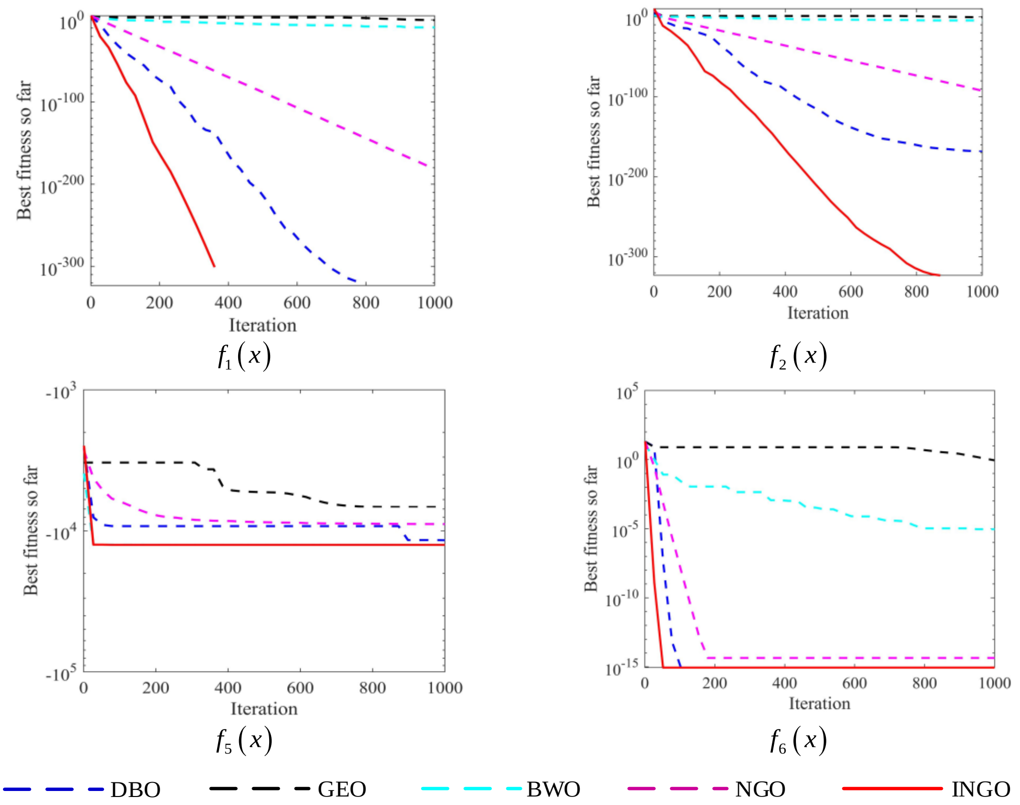

Fig. 4. Convergence curves of the algorithm under the four test functions.

3.1.3. INGO-VMD parameter optimization process

INGO algorithm is used to optimize the VMD decomposition parameters. In the whole process of optimization, the selection of fitness function plays a crucial role in the optimization results. The entropy value can be used to measure the complexity of a signal, that is, the more sparse the signal is, the more fault feature information, and the less the entropy value. Therefore, the envelope entropy is used as the fitness function to optimize the VMD parameters in this section, and its envelope entropy is defined as follows:

$$p_j = a(j)/\sum_{j=1}^{N} a(j)\, E_p = -\sum_{j=1}^{N} p_j \lg p_j \tag{14}$$

Where, $a(j)$ is the envelope signal of each component after Hilbert demodulation, and $a(j)$ is the normalized form of p_j.

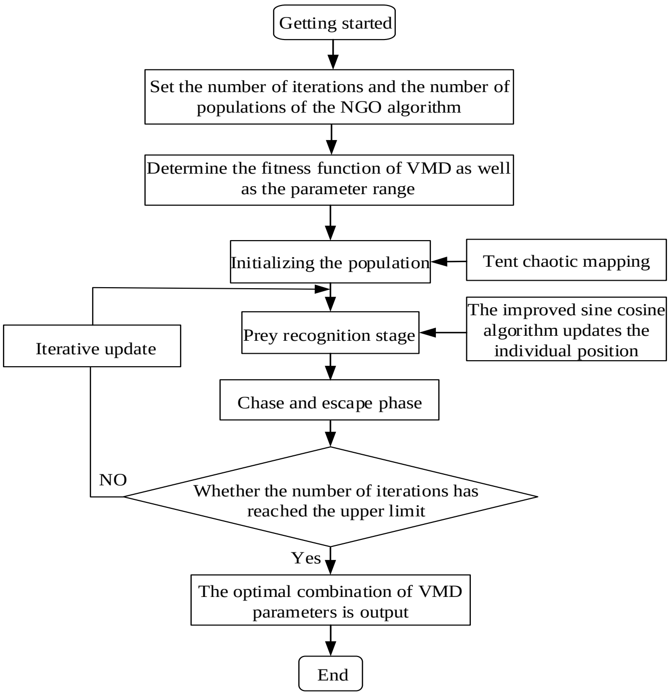

Fig. 5. Flow chart of INGO optimizing VMD parameters.

Based on the above research, the flow chart of INGO algorithm to optimize VMD is shown in Fig. 5.

3.2. Construction of the lead screw wear feature fusion data set

INGO was used to optimize the VMD parameters to obtain the optimal parameter k and α, and the optimal parameter combination was used to decompose the vibration signal into IMFs components. Some of these IMFs components contained important information about the wear state of the ball screw, while the other part may be interfered by background noise. Therefore, these noise interference components need to be eliminated in order to accurately extract the wear characteristics of the ball screw. The correlation coefficient method can reflect the correlation between signals; in general, the larger the value, the greater the correlation degree, and the less noisy information in the IMF component. Therefore, in this paper, the correlation coefficient method is used to screen the effective IMF components, so as to achieve the effect of noise reduction. It is calculated as follows:

$$r = \frac{\sum_{i=1}^{n}(x_i - \bar{x})(y_i - \bar{y})}{\sqrt{\sum_{i=1}^{n}(x_i - \bar{x})^2 \sum_{i=1}^{n}(y_i - \bar{y})^2}} \tag{15}$$

Where, x_i is the original vibration signal, $i = 1,2,\cdots,n$, y_i are the IMF components obtained by VMD decomposition.

For the filtered IMF components, the multi-feature quantization method of calculating power spectral entropy[35], permutation entropy[36] and fuzzy entropy[37] fusion was proposed. Among them, the power spectrum entropy is extracted from the frequency domain feature of the signal, and the smaller the power spectrum entropy value is, the greater the wear degree is. The permutation entropy can well amplify the micro-variation signal of the system and detect the dynamic mutation of the complex system, so its characteristics can reflect the weak change of the wear state. As for the fuzzy entropy feature, it has strong sensitivity to the slight disturbance of the signal, and can be used to characterize the change of signal complexity related to the wear state. Combined with the above analysis, the power spectral entropy, permutation entropy and fuzzy entropy of all IMF components after optimization are extracted, and the multi-feature fusion sample data set of the lead screw is finally constructed.

4. Recognition method of wear state of lead screw based on BO-BiLSTM

On the basis of extracting the wear features of the lead screw, a suitable wear state classification and recognition method is needed to classify and identify the extracted features. BiLSTM algorithm has the advantages of strong learning ability and high classification and recognition accuracy. Therefore, the BiLSTM algorithm is applied to identify the wear state of the lead screw in this paper.

4.1. Improvement of BiLSTM algorithm

BiLSTM is an improved algorithm based on LSTM algorithm, which is a bidirectional recurrent neural network composed of forward LSTM and backward LSTM. It can simultaneously model the input data from both forward and backward directions, and can obtain context and future information. Its principle and calculation steps are detailed in reference[38]. However, when applying the BiLSTM algorithm, the value of the hyperparameter will directly affect the performance and recognition effect of the model. Bayesian algorithm is an effective tool in the field of fault diagnosis [39, 40], As a global optimization algorithm, it can find the optimal combination of hyperparameters of the current model.Therefore, in this paper, the hyperparameter combination of Bayesian Optimization (BO) BiLSTM model is adopted.The basic idea is to quickly evaluate the objective function based on Bayes theorem to update the posterior distribution of the optimization function, and then select the next optimal hyperparameter combination to sample according to the distribution.

Let the combination of hyperparameters to be optimized be $X = \{x_1, x_2, \cdots, x_n\}$. When selecting the combination of hyperparameters, the following formula can be used to solve the problem:

$$x_{opt} = argmin\, f(x), x \in X \tag{16}$$

Where, x_{opt} is the optimal combination of hyperparameters of the BiLSTM model, $f(x)$ is the objective function to minimize the performance of the evaluation model, and the mean square error (MSE) of the BiLSTM model recognition results is used as the objective function of Bayesian optimization, and its formula is as follows:

$$MSE = \frac{1}{N}\sum_{i=1}^{N}(y_i - \hat{y})^2 \tag{17}$$

Where, N is the number of sample groups, y_i is the true value, and $\hat{y}$ is the identified value.

The core of Bayesian optimization is mainly divided into two parts, the first is the probabilistic surrogate model, and the second is the acquisition function. The choice of an appropriate probabilistic surrogate model and acquisition function is related to the effect of optimization. In this paper, the Gaussian process surrogate model and EI function are used to construct the Bayesian optimization algorithm, and the construction result of the posterior distribution is obtained according to the observed data set, and then the next point to be evaluated is selected through the EI function, and then the prior knowledge is iteratively corrected to improve the accuracy of the Gaussian surrogate model, and finally the optimal combination of hyperparameters is found.

5. Wear state recognition implementation and result analysis

5.1. INGO-VMD decomposition and feature extraction

In the process of using INGO to optimize VMD, the minimum envelope entropy is used as the fitness function of INGO to determine the parameter combination of VMD decomposition. In this paper, the ball screw wear sample signal shown in Fig. 2(c) is taken as an example to conduct the optimization experiment of VMD parameters, and the maximum number of iterations is set to 1000, the number of populations is 110, the value range of k is [2,10], and the value of α is [10,5000]. The fitness iteration curve is shown in Fig. 6.

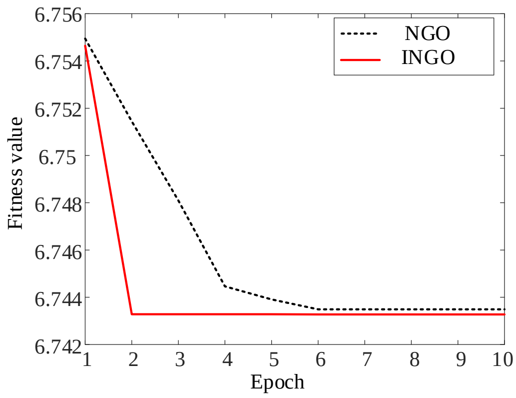

Fig. 6. Fitness iteration curve of VMD parameter optimization.

It can be seen from Figure 6 that INGO optimizes the VMD iteration to the second time and the fitness value remains stable for eight consecutive times thereafter, at which point the combination of k and α is [6,1560], while the fitness value of NGO optimizes the VMD algorithm only reaches the minimum in the sixth iteration, indicating that INGO has a faster convergence speed than NGO. The VMD decomposition was performed using the optimal combination and the results are shown in Fig. 7.

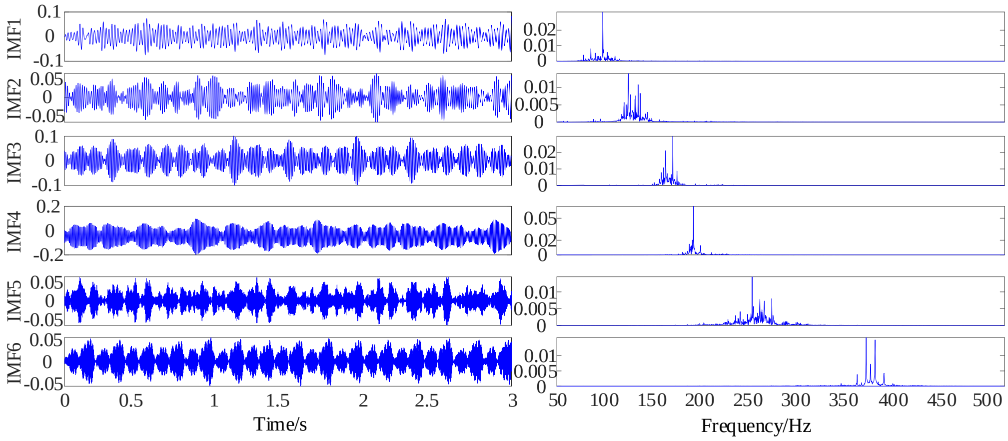

Fig .7. Time-frequency plot of INGO-VMD decomposition.

The left part of Fig. 7 shows the time domain waveform diagram of each component, and the right part shows the corresponding spectrogram of each component. It can be seen that the frequency distribution of each IMF component is uniform, and there is no mode aliasing. Therefore, it can be shown that the method decomposed by INGO-VMD has good decomposition effect. Other sample signals were analyzed by the same method, and 600 groups of sample signals were obtained.

After the IMFs components are decomposed, the correlation coefficient method is used to eliminate the false components that are not related to the wear characteristics. The correlation coefficient calculation results between each IMF component and the original signal are shown in Table 3.

Table 3. Correlation coefficients between IMF components and original signals.

IMF component	IMF1	IMF2	IMF3	IMF4	IMF5	IMF6
Coefficient of correlation	0.7761	0.4053	0.5489	0.4962	0.2985	0.3219

As can be seen from the results in Table 3, the correlation coefficient of IMF1-1MF4 is larger than that of IMF5 and IMF6, that is, the first four components are most similar to the original signal, that means the first four components contain less noise. The power spectral entropy, permutation entropy and fuzzy entropy of the four IMF components after screening were calculated, and a 600×12 dimensional lead screw wear feature data set was constructed. The samples of each wear state in this data set were divided, and 30% were randomly selected as the test data set and the remaining 70% as the training data set.

5.2. Implementation of wear state identification

After splitting the dataset, we then apply Bayesian optimization to the hyperparameters in the BiLSTM model, with the MSE value as the objective function to minimize it. The maximum number of iterations of the hyperparameters of the Bayesian optimization network model was set to 30, and the optimization was stopped when the number of iterations reached the maximum, and the best combination of hyperparameters was output. The BiLSTM model hyperparameter Settings are shown in Table 4.

Table 4 Hyperparameter Settings of BiLSTM model

parameters	Parameter values
α	0.005
hidden_layer_unit	20
epochs	150
batch_size	8
optimizer	Adam
dropout	0.1
inputsize	12
numclasses	5

The wear feature data set and the hyperparameter combination of the Bayesian optimized BiLSTM model were input to construct a model based on INGO-VMD-BO-BiLSTM. This model was applied to compare with the network model before Bayesian optimization for wear state identification, and the final training results of the two models were shown in Fig. 8.

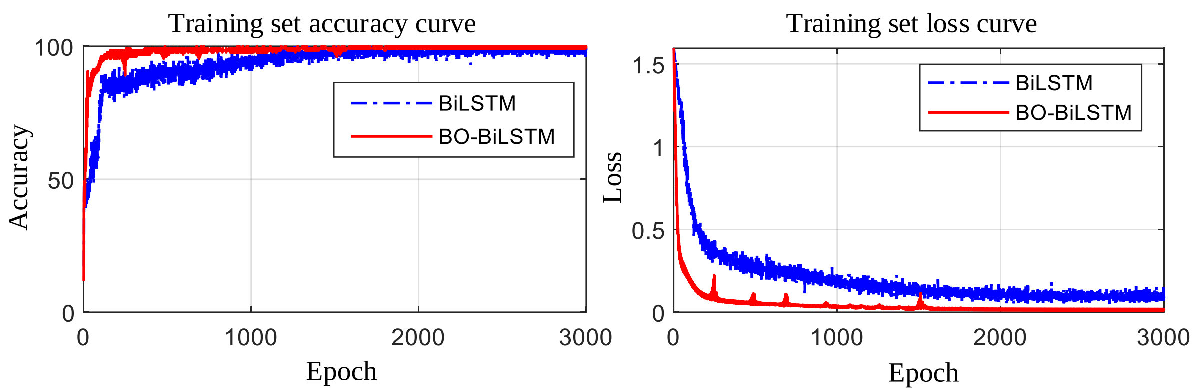

Fig. 8. Comparison of accuracy and training loss before and after model improvement.

Fig. 8 shows that as the number of iterations increases, the accuracy of the two models on the training set also increases, but the BO-BiLSTM model is able to converge in fewer iterations and has higher accuracy than the BiLSTM model. At the same time, the loss function value of the BO-BiLSTM model decreases faster than that of the BiLSTM model, and it can also stably converge to a very small error in a short number of iterations. In summary, the recognition analysis of the two models shows that after the BiLSTM model is introduced into the Bayesian network, the recognition accuracy of the model has been greatly improved.

In order to further verify the superiority of the proposed method, 180×12 dimensional feature test samples are input into the VMD-LSTM, VMD-BiLSTM, and VMD-BO-BiLSTM models for testing. Among them, the number of modes of VMD is artificially selected as k =3, the penalty factor α =2500, and the other parameters are set consistently. The wear state classification and recognition results of the ball screw element action unit based on the four models are shown in Fig. 9.

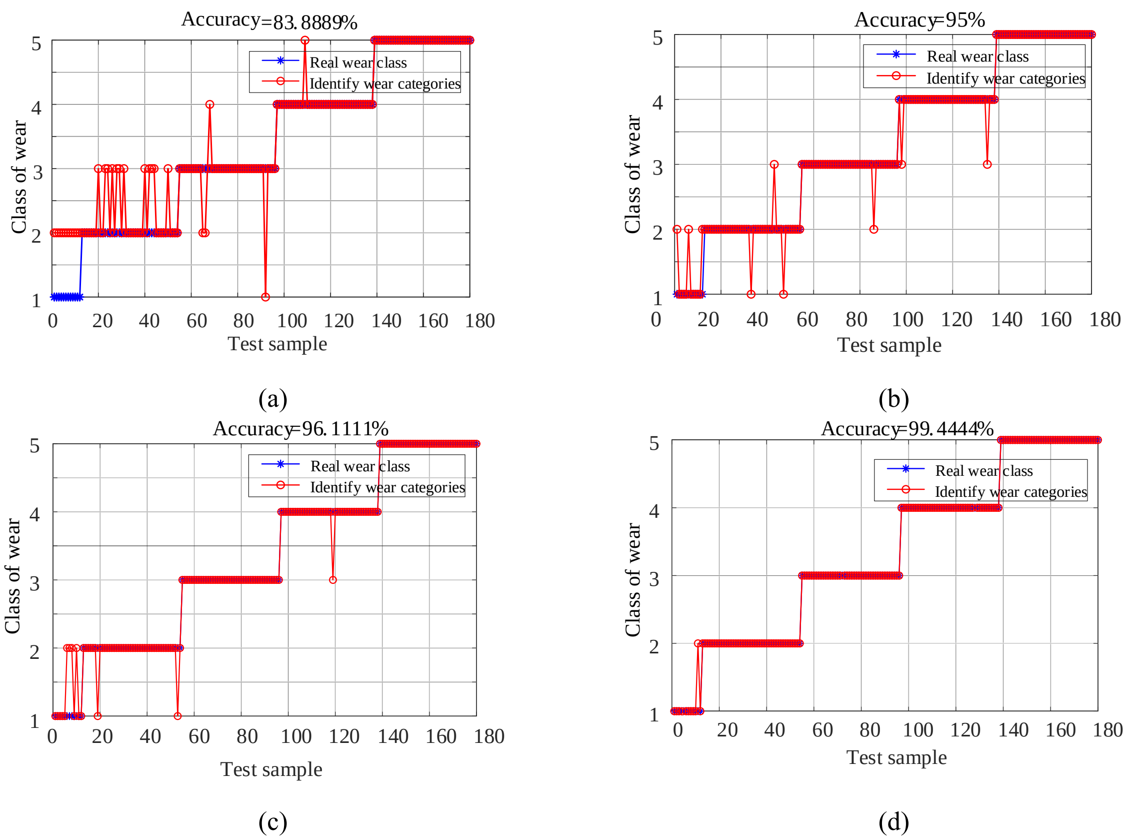

Fig. 9. Wear state identification results of four models

Figure 9(a), 9(b) and 9(c) show the recognition results after the feature test samples were input into the VMD-LSTM, VMD-BiLSTM, and VMD-BO-BiLSTM models, respectively, and the recognition accuracy rates obtained are 83.8889%, 95% and 96.1111%. The number of errors in the corresponding samples was 29,9, and 7 respectively. As can be seen from Fig. 9(d), in the recognition results of the application of INGO-VMD-BO-BiLSTM model, only one sample in good health was wrongly identified as the initial wear state, and the recognition accuracy rate of the rest wear states was 100%, and the overall recognition accuracy rate on the obtained test set was as high as 99.4444%. Compared with VMD-LSTM, VMD-BiLSTM, and VMD-BO-BiLSTM models, the recognition accuracy is improved by 15.5555%, 4.4444% and 3.3333%, respectively. Therefore, the wear state recognition method proposed in this paper based on INGO-VMD and Bayesian optimization BiLSTM model can accurately identify different wear states of ball screw, and through comparison with other methods, the proposed method has certain feasibility and superiority.

6. Conclusion

Aiming at the problem that it is difficult to extract the wear characteristic information of the ball screw meta-action unit middleware screw under noise interference, this paper proposes a wear state recognition method based on INGO algorithm optimization VMD and Bayesian optimization BiLSTM model. The main conclusions are as follows:

(1) Tent chaotic map and adaptive weight sine cosine algorithm are introduced into NGO algorithm. Through the comparison of optimization ability, it is verified that INGO algorithm has better convergence accuracy and faster convergence speed. Then, the INGO algorithm is used to optimize the number of modes k and the penalty factor α of VMD. The results show that the INGO-VMD decomposition method can effectively avoid the mode mixing problem caused by improper parameter setting.

(2) INGO-VMD and Bayesian optimized BiLSTM are used to realize the recognition of five wear states of the lead screw, and the recognition and classification accuracy is as high as 99.4444%. By further comparison with other models, the feasibility and superiority of the designed method in this paper are verified.

(3) This paper focuses on the wear of the leading screw, which is the most prominent part of the wear of the ball screw meta-action unit, and realizes the wear state identification of the leading screw through the application of a series of methods. Subsequently, the designed method can be applied to the wear state identification of other components of the ball screw element action unit, so as to improve the specific practical application of the designed method.

References

1. Li, Y.; Li, J.; Liu, S.; Wen, S.; Li, D.; Zhang, G., Meta-action unit importance identification method of electromechanical product. *Proceedings of the Institution of Mechanical Engineers Part C-Journal of Mechanical Engineering Science* 2022, 236, (16), 9027-9036. doi: 10.1177/09544062221091776.
2. Li, Y.; Zhang, X.; Ran, Y.; Zhang, W.; Zhang, G., Reliability and Modal Analysis of Key Meta-Action Unit for CNC Machine Tool. *Ieee Access* 2019, 7, 23640-23655. doi: 10.1109/access.2019.2899623.
3. Shan, P.; Lv, H.; Yu, L.; Ge, H.; Li, Y.; Gu, L., A Multisensor Data Fusion Method for Ball Screw Fault Diagnosis Based on Convolutional Neural Network With Selected Channels. *Ieee Sensors Journal* 2020, 20, (14), 7896-7905. doi: 10.1109/jsen.2020.2980868.
4. Pandhare, V.; Miller, M.; Vogl, G. W.; Lee, J., Ball Screw Health Monitoring With Inertial Sensors. *Ieee Transactions on Industrial Informatics* 2023, 19, (6), 7323-7334. doi: 10.1109/tii.2022.3210999.
5. Zhang, X.; Luo, T.; Han, T.; Gao, H., A novel performance degradation prognostics approach and its application on ball screw. *Measurement* 2022, 195. doi: 10.1016/j.measurement.2022.111184.
6. Jia, P.; Rong, Y.; Huang, Y., Condition monitoring of the feed drive system of a machine tool based on long-term operational modal analysis. *International Journal of Machine Tools & Manufacture* 2019, 146. doi: 10.1016/j.ijmachtools.2019.103454.
7. Butler, Q.; Ziada, Y.; Stephenson, D.; Gadsden, S. A., Condition Monitoring of Machine Tool Feed Drives: A Review. *Journal of Manufacturing Science and Engineering-Transactions of the Asme* 2022, 144, (10). doi: 10.1115/1.4054516.
8. Yi-Cheng, H.; Yi-Keng, H., Applying a support vector machine for hollow ball screw condition-based classification using feature extraction. *Proceedings of the Institution of Mechanical Engineers* 2022, 236, (14), 1839-1852. doi:10.1177/0954405420958842.

9. Benker, M.; Zaeh, M. F., Condition monitoring of ball screw feed drives using convolutional neural networks. *Cirp Annals-Manufacturing Technology* 2022, 71, (1), 313-316. doi: 10.1016/j.cirp.2022.03.017.
10. Li, R.; Wei, P.; Liu, X.; Li, C.; Ni, J.; Zhao, W.; Zhao, L.; Hou, K., Cutting tool wear state recognition based on a channel-space attention mechanism. *Journal of Manufacturing Systems* 2023, 69, 135-149. doi: 10.1016/j.jmsy.2023.06.010.
11. Xue, Y.-J.; Cao, J.-X.; Wang, D.-X.; Du, H.-K.; Yao, Y., Application of the Variational-Mode Decomposition for Seismic Time-frequency Analysis. *Ieee Journal of Selected Topics in Applied Earth Observations and Remote Sensing* 2016, 9, (8), 3821-3831. doi: 10.1109/jstars.2016.2529702.
12. Zhang, Y.; Qi, X.; Wang, T.; He, Y., Tool Wear Condition Monitoring Method Based on Deep Learning with Force Signals. *Sensors* 2023, 23, (10). doi: 10.3390/s23104595.
13. Xie, Z.; Yu, D.; Zhan, C.; Zhao, Q.; Wang, J.; Liu, J.; Liu, J., Ball screw fault diagnosis based on continuous wavelet transform and two-dimensional convolution neural network. *Measurement & Control* 2023, 56, (3-4), 518-528. doi: 10.1177/00202940221107620.
14. Lee, W. G.; Lee, J. W.; Hong, M. S.; Nam, S.-H.; Jeon, Y.; Lee, M. G., Failure Diagnosis System for a Ball-Screw by Using Vibration Signals. *Shock and Vibration* 2015, 2015. doi: 10.1155/2015/435870.
15. Jinde, Z.; Miaoxian, S.; Wanming, Y.; Jinyu, T.; Ziwei, P., Improved uniform phase empirical mode decomposition and its application in machinery fault diagnosis. *Measurement* 2021, 179. doi: 10.1016/j.measurement.2021.109425.
16. Feng, Z.; Zhang, D.; Zuo, M. J., Adaptive Mode Decomposition Methods and Their Applications in Signal Analysis for Machinery Fault Diagnosis: A Review With Examples. *Ieee Access* 2017, 5, 24301-24331. doi: 10.1109/access.2017.2766232.
17. Zhenzhen, J., Research on fault diagnosis method of bearing based on parameter optimization VMD and improved DBN. *Journal of Vibroengineering* 2023, 25, (6), 1068-1082. doi: 10.1016/j.acme.2016.05.003.
18. Zhao, H.; Liu, H.; Xu, J.; Guo, C.; Deng, W., Research on a fault diagnosis method of rolling bearings using variation mode decomposition and deep belief network. *Journal of Mechanical Science and Technology* 2019, 33, (9), 4165-4172. doi: 10.1007/s12206-019-0811-2.
19. Dragomiretskiy, K.; Zosso, D., Variational Mode Decomposition. *IEEE Trans. Signal Processing* 2014, 62, (3), 531-544. doi: 10.1109/TSP.2013.2288675.
20. Zhang, X.; Zhao, J., COMPOUND FAULT DETECTION IN GEARBOX BASED ON TIME SYNCHRONOUS RESAMPLE AND ADAPTIVE VARIATIONAL MODE DECOMPOSITION. *Eksploatacja I Niezawodnosc-Maintenance and Reliability* 2020, 22, (1), 161-169. doi: 10.17531/ein.2020.1.19.
21. Ziyou, Z.; Wenhua, C.; Ce, Y., Adaptive range selection for parameter optimization of VMD algorithm in rolling bearing fault diagnosis under strong background noise. *Journal of Mechanical Science and Technology* 2023, 37, (11), 5759-5773. doi: 10.1007/s12206-023-1015-3.
22. Li, G.; Deng, H.; Yang, H., Traffic flow prediction model based on improved variational mode decomposition and error correction. *Alexandria Engineering Journal* 2023, 76, 361-389. doi: 10.1016/j.aej.2023.06.008.
23. Xu, F. J.; Jing, R. R.; Zhang, Y.; Liu, Q.; Wu, Y. A., High accuracy key feature extraction approach for the non-stationary signals measurement based on NGO-VMD noise reduction and CNN-LSTM. *Measurement Science and Technology* 2024, 35, (1). doi: 10.1088/1361-6501/ad031c.
24. Li, K.; Huang, H. S.; Fu, S. W.; Ma, C.; Fan, Q. S.; Zhu, Y. W., A multi-strategy enhanced northern goshawk optimization algorithm for global optimization and engineering design problems. *Computer Methods in Applied Mechanics and Engineering* 2023, 415. doi: 10.1016/j.cma.2023.116199.
25. Laddada, S.; Si-Chaib, M. O.; Benkedjouh, T.; Drai, R., Tool wear condition monitoring based on wavelet transform and improved extreme learning machine. *Proceedings of the Institution of Mechanical Engineers, Part C: Journal of Mechanical Engineering Science* 2020, 234, (5), 1057-1068. doi: 10.1177/0954406219888544.
26. Ou, J.; Li, H.; Huang, G.; Yang, G., Intelligent analysis of tool wear state using stacked denoising autoencoder with online sequential-extreme learning machine. *Measurement* 2021, 167. doi: 10.1016/j.measurement.2020.108153.
27. Zhang, B. C.; Sun, S. Q.; Yin, X. J.; He, W. D.; Gao, Z., Research on Gearbox Fault Diagnosis Method Based on VMD and Optimized LSTM. *Applied Sciences-Basel* 2023, 13, (21). doi: 10.3390/app132111637.
28. Liang, T.; Meng, Z.; Xie, G.; Fan, S., Multi-Running State Health Assessment of Wind Turbines Drive System Based on BiLSTM and

GMM. *Ieee Access* 2020, 8, 143042-143054. doi: 10.1109/access.2020.3014371.

29. Wu, Z.; Wang, Z.; Wei, H.; Ren, J.; Yuan, Y.; Wang, T.; Duan, W.; Wei, H.; Wang, S., Remaining useful life prediction for equipment based on RF-BiLSTM. *Aip Advances* 2022, 12, (11). doi: 10.1063/5.0125885.
30. Jinsong, Z.; Jingbo, P.; Weixuan, W.; Shuaiguo, L., Aeroengine Working Condition Recognition Based on MsCNN-BiLSTM. *Sensors* 2022, 22, (18), 7071-7071. doi: 10.3390/s22187071.
31. Chen, Q. P.; Xie, Q. S.; Yuan, Q. N.; Huang, H. S.; Li, Y. T., Research on a Real-Time Monitoring Method for the Wear State of a Tool Based on a Convolutional Bidirectional LSTM Model. *Symmetry-Basel* 2019, 11, (10). doi: 10.3390/sym11101233.
32. Zhaosu, L.; Jianfeng, Y., Research on Short-term Load Forecasting Based on GWO-BILSTM. *Journal of Physics: Conference Series* 2022, 2290, (1). doi: 10.1088/1742-6596/2290/1/012100.
33. M., L. A.; M., d. S. L. F.; M., d. S. C.; Yulong, L.; Junfa, L.; Shengquan, L.; Shutao, W.; Donglong, L.; Genbao, Z., Meta-action unit importance identification method of electromechanical product. *Proceedings of the Institution of Mechanical Engineers, Part C: Journal of Mechanical Engineering Science* 2022, 236, (16), 9027-9036. doi: 10.1177/09544062221091776.
34. Dehghani, M.; Hubalovsky, S.; Trojovsky, P., Northern Goshawk Optimization: A New Swarm-Based Algorithm for Solving Optimization Problems. *Ieee Access* 2021, 9, 162059-162080. doi: 10.1109/access.2021.3133286.
35. Zheng, Z.; Xin, G., Fault Feature Extraction of Hydraulic Pumps Based on Symplectic Geometry Mode Decomposition and Power Spectral Entropy. *Entropy* 2019, 21, (5). doi: 10.3390/e21050476.
36. Sun, H.; Wu, C.; Liang, X.; Zeng, Q., Identification of Multiple Faults in Gearbox Based on Multipoint Optional Minimum Entropy Deconvolution Adjusted and Permutation Entropy. *Entropy* 2018, 20, (11). doi: 10.3390/e20110850.
37. Minhas, A. S.; Sharma, N.; Singh, G.; Kankar, P. K.; Singh, S., Improvement in classification accuracy and computational speed in bearing fault diagnosis using multiscale fuzzy entropy. *Journal of the Brazilian Society of Mechanical Sciences and Engineering* 2020, 42, (11). doi: 10.1007/s40430-020-02671-1.
38. Xing, X.; Chengxing, L.; Yun, Z.; Xiaoshu, L., Short - term traffic flow prediction based on whale optimization algorithm optimized BiLSTM_Attention. *Concurrency and Computation: Practice and Experience* 2022, 34, (10). doi: 10.1002/cpe.6782.
39. Chao, Y.; Baoping, C.; Rui, Z.; Zhexian, Z.; Xiangdi, K.; Xiaoyan, S.; Yiliu, L.; Haidong, S.; Javed, A. K., Cross-validation enhanced digital twin driven fault diagnosis methodology for minor faults of subsea production control system. *Mechanical Systems and Signal Processing* 2023, 204. doi: 10.1016/J.YMSSP.2023.110813
40. Yang, C.; Cai, B. P.; Wu, Q. B.; Wang, C. Y. S.; Ge, W. F.; Hu, Z. M.; Zhu, W.; Zhang, L.; Wang, L. T., Digital twin-driven fault diagnosis method for composite faults by combining virtual and real data. Journal of Industrial Information Integration 2023, 33. doi:10.1016/j.jii.2023.100469.